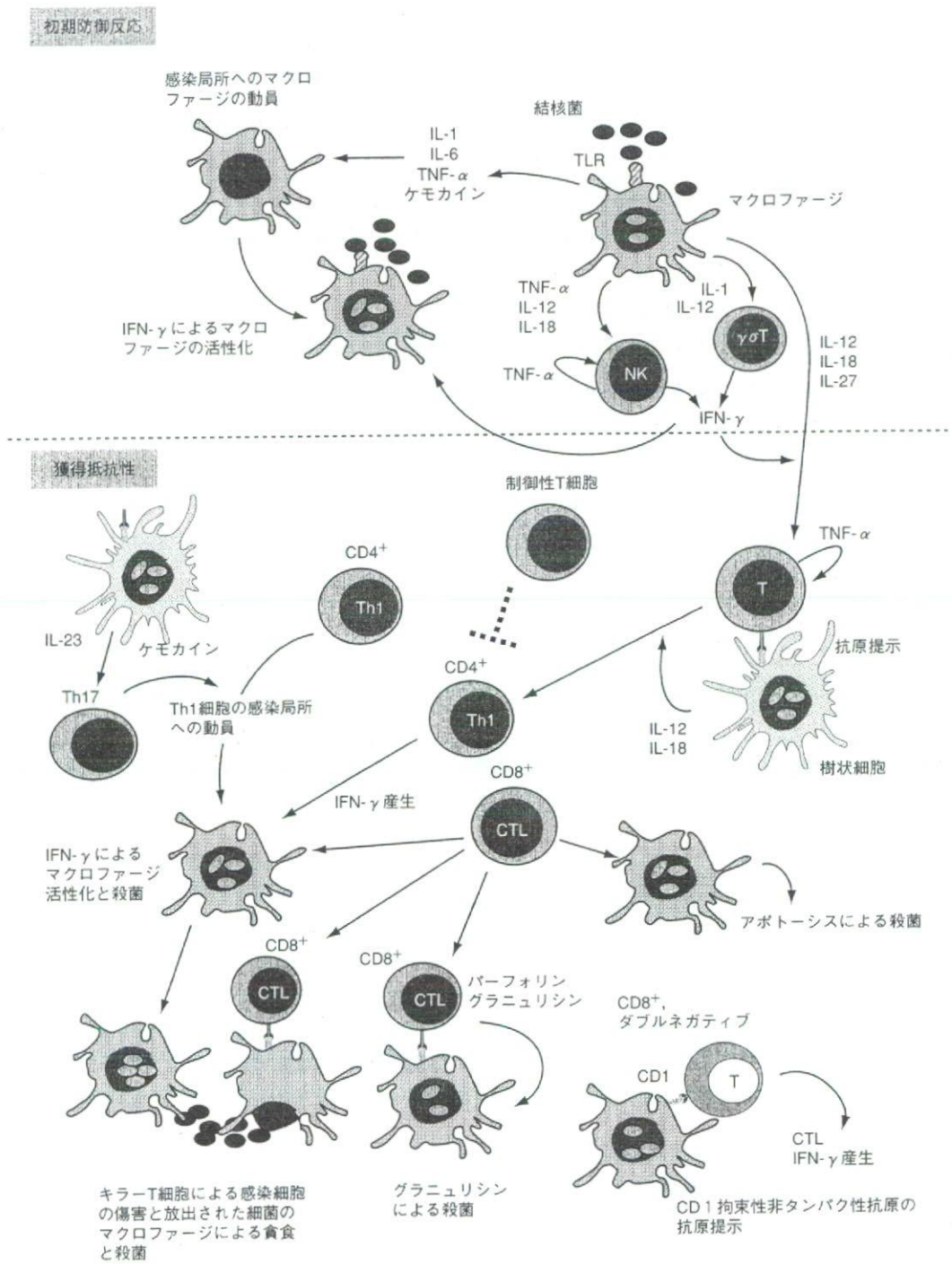

図2　抗結核防御免疫発現のメカニズム

マクロファージはTLRを介して結核菌を認識し，炎症性サイトカインやケモカインを産生してマクロファージおよびT細胞を感染局所に動員する．また，マクロファージが産生するIL-12，IL-18，IL-1およびTNF-αは，NK細胞およびγδT細胞に作用して初期防御に重要なIFN-γ産生を誘導する．IFN-γはマクロファージの細胞内殺菌能を増強するとともにIFN-γ産生性$CD4^+$T細胞の分化を誘導する．抗原特異的$CD8^+$T細胞は，大量のIFN-γを産生するだけでなく，グラニュリシンの産生あるいは感染細胞にアポトーシスを誘導することにより菌を排除する．CD1拘束性に非タンパク性抗原を提示されたT細胞はキラー活性およびIFN-γ産生を介して防御免疫に関与する．また，Th17細胞はケモカインを産生し，IFN-γ産生性T細胞の感染局所に動員する．さらに，この感染防御免疫の発現は，制御性T細胞による制御を受けている

文献

1) Cole, S. T. et al.：Nature, 393：537-544, 1998
2) Crevel, R. V. et al.：Clin. Microbiol. Rev., 15：294-309, 2002
3) Nigou, J. et al.：J. Immunol., 166：7477-7485, 2001
4) Malik, Z. A. et al.：J. Exp.Med., 191：287-302, 2000
5) Kohwiwattanagun, J. et al.：Microbiol. Immunol., 51：253-261, 2007
6) Aoki, K. et al.：J. Biol. Chem., 279：39798-39806, 2004
7) Deretic, V. et al.：Cell Microbiol., 8：719-727, 2006
8) Jayachandran, R. et al.：Cell, 130：37-50, 2007
9) Gutierrez, M. G. et al.：Cell, 119：753-766, 2004
10) Schmid, D. & Munz, C.：Immunity, 27：11-21, 2007
11) Sly, L. M. et al.：J. Immunol., 170：430-437, 2003
12) Spira, A. et al.：Am. J. Respir. Cell Mol. Biol., 29：545-551, 2003
13) Wayne, L. G. & Sohaskey, C. D.：Annu. Rev. Microbiol., 55：139-163, 2001
14) McKlnney, J. D. et al.：Nature, 406：735-738, 2000
15) Kaku, T. et al.：FEMS Microbiol. Lett., 274：189-195, 2007
16) Uchiyama, R. et al.：Infect. Immun. 75：2894-2902, 2007
17) Lopez, M. et al.：J. Immunol., 170：2409-2416, 2003
18) Xu, Y. et al.：Immunity, 27：135-144, 2007
19) Means, T. K. et al.：J. Immunol., 163：3920-3927, 1999
20) Wolf, A. J. et al.：J. Immunol., 179：2509-2519, 2007
21) Stenger, S. et al..：Science, 282：121-125, 1998
22) Schaible, U. E. et al.：Trend Microbiol., 8：419-425, 2000
23) Khader, S. A. et al.：Nat. Immunol., 8：369-377, 2007
24) Lockhart, E. et al.：J. Immunol., 177：4662-4669, 2006
25) Kursar, M. et al.：J. Immunol., 178：2661-2665, 2007

<筆頭著者プロフィール>

河村 伊久雄：1989年九州大学大学院医学系研究科博士過程を修了し，新潟大学医学部細菌学助手に採用される．'95～'97年に米国コーネル大学およびカリフォルニア大学バークレー校に留学．Dr. Lee W. Rileyの研究室で，結核菌の侵入因子Mce1について研究を行う．'98年より京都大学医学研究科微生物感染症学助手，2004年同助教授になる．現在，結核菌およびリステリアの病原性と感染防御免疫誘導能の関係について研究を行っている．

J Neuropathol Exp Neurol

Vol. 66, No. 4
April 2007
pp. 284–294

ORIGINAL ARTICLE

Mycobacterium leprae in Neurons of the Medulla Oblongata and Spinal Cord in Leprosy

Thida Aung, MBBS, MSc, Shinichi Kitajima, MD, PhD, Mitsuharu Nomoto, MD, PhD, Junichiro En, MA, Suguru Yonezawa, MD, PhD, Isao Arikawa, MD, and Masamichi Goto, MD, PhD

Abstract

Peripheral neuropathy has been extensively studied in leprosy, a chronic disease caused by *Mycobacterium leprae*, but the central nervous system (CNS) is thought to be free from bacilli. Involvement of the CNS was explored in autopsy cases of clinically cured lepromatous leprosy (n = 67) and in non-leprosy cases (n = 15). Paraffin sections of the medulla oblongata and spinal cord were subjected to hematoxylin and eosin staining, Fite acid-fast staining, and anti-phenolic glycolipid-I (PGL-I) immunostaining. PGL-I-positive areas were microdissected from selected cases and nested polymerase chain reaction (PCR) targeting the *M. leprae*-specific repetitive sequence was performed. Of the 67 cases of leprosy, 44 (67%) had vacuolar changes of motor neurons either in medulla oblongata (nucleus ambiguus or hypoglossal nucleus) or spinal cord. Fite staining was negative, but PGL-I was positive in vacuolated areas. PCR revealed *M. leprae*-specific genomic DNA in 18 of 19 cases (95%) with vacuolated changes and 5 of 8 (63%) without vacuolated changes. All of above findings were negative in control cases. Terminal deoxynucleotidyl transferase dUTP nick-end labeling staining did not show a significant increase of apoptosis in the neurons. The PCR positivity had a significant correlation with PGL-I immunostaining ($p < 0.05$). The presence of vacuolar changes in the spinal cord was correlated with hand and feet deformity grades ($p = 0.04$). This study provides significant additional evidence to indicate that *M. leprae* is present in the CNS in a subset of patients. Further investigation is required to correlate this finding to motor dysfunction and silent neuropathy in leprosy.

Key Words: Central nervous system, Immunohistochemistry, Leprosy, *Mycobacterium leprae*, Neuropathy, Polymerase chain reaction

From the Department of Human Pathology, Field of Oncology (TA, MN, JE, SY, MG), Kagoshima University Graduate School of Medical and Dental Sciences, Kagoshima, Japan; Department of Pathology (TA), University of Medicine (1), Yangon, Myanmar; Department of Pathology (SK), Kagoshima University Hospital, Kagoshima, Japan; and the National Hansen Disease Hospital (JE, IA), Hoshizuka-Keiaien, Kagoshima, Japan.

Send correspondence and reprint requests to: Masamichi Goto, MD, Department of Human Pathology, Field of Oncology, Kagoshima University Graduate School of Medical and Dental Sciences, 8-35-1, Sakuragaoka, Kagoshima 890-8544, Japan; E-mail: masagoto@m2.kufm.kagoshima-u.ac.jp

This work was supported by grants from the U.S.-Japan Cooperative Medical Science Program and an International Cooperation Research Grant from the International Medical Center of Japan.

A supplementary figure is available online at http://www.jneuropath.com.

INTRODUCTION

Leprosy is a chronic, infectious, neurodegenerative human disease caused by *Mycobacterium leprae* and is still a major global health problem: approximately 410,000 new cases of leprosy were detected in 2004, and at the beginning of 2005 approximately 290,000 leprosy patients were receiving treatment (1). Although multidrug therapy has had a dramatic impact on global prevalence, there are still 2 to 3 million people worldwide with deformities due to leprosy. Thus, detection, management, and understanding of the mechanisms involved in nerve damage in leprosy remain as high priorities (2). Neurotropism and involvement of *M. leprae* in the peripheral nervous system have been commonly reported as a cause of neuropathy, but less attention has been paid to central nervous system (CNS) damage in patients with leprosy, despite several reports of this phenomenon (3–5). Koya and Arakawa examined the spinal cord of leprosy (lepromatous, 8 cases; tuberculoid, 4 cases) and found marked degeneration of the posterior column, especially the gracile fasciculus (3). However, Harada's highly sensitive acid-fast staining (6) was negative in the motor neurons of anterior horns (3). Yamada (5) examined the brain and spinal cord of 173 leprosy cases (lepromatous, n = 133; tuberculoid, n = 36, other type, n = 4) by Harada's method (6) and found numerous leprous para-rosanilin-positive material (LLPM) in the periaxonal spaces of cerebrum (28%), medulla oblongata (32%), and spinal cord (7%). LLPM was observed in 36% of lepromatous leprosy and 42% of tuberculoid leprosy, and the progressive stage of leprosy shows a lower positive rate (27%) than that seen in the quiescent stage (40%). He also did not observe LLPM in neuronal soma (5). Furthermore, the human brain and spinal cord have been considered to be free from bacilli in leprosy. However, Mitsuda described the presence of acid-fast bacilli in the neurons of the spinal cord and medulla oblongata in 1952 (7), and we also demonstrated *M. leprae*-specific phenolic glycolipid-I (PGL-I)-positive substances in such neurons in a pilot study (8).

In leprosy, nerve damage and paralysis are most often associated with an attack of acute or subacute neuritis, which occurs as part of the reaction episode (9). Srinivasan et al (10) observed that nerve trunks often become paralyzed quietly without such manifestations and suggested that this is probably the most common mode of onset of nerve-trunk paralysis; hence, the term quiet nerve paralysis was proposed

for this condition. Out of 500 high-risk patients, 58 developed motor paralysis over a period of 2 years, and in 47 of these patients (81%) the onset of paralysis was not associated with a remembered episode of neuritis in the affected nerve trunk (9). In a series of 108 patients with pure neuritic leprosy, Kaur et al (11) found that 34 had motor paralysis or paralysis and deformity, and approximately 70 had sensory loss limited to the distribution of nerve trunks; however, only 5 of 108 patients were reported to have nerve pain. The terms silent neuritis and silent neuropathy are also used to refer to quiet nerve paralysis (12, 13).

To date, the exact etiology and pathogenesis of motor paralysis in leprosy have not been identified. However, degeneration of motor neurons occurs in patients with motor neuron diseases such as amyotrophic lateral sclerosis, and we looked for similar nerve damage in leprosy in this study.

MATERIALS AND METHODS

Case Selection

The study was approved by the Human Investigation Committee, Faculty of Medicine, Kagoshima University. Ninety-six autopsies were performed in the National Hansen Disease Hospital Hoshizuka-Keiaien, Kagoshima, Japan, from 1990 to 2000, among which were 67 cases with a history of lepromatous leprosy. Most of these cases were negative for mycobacteria in a slit skin smear test when they died, and these cases of cured lepromatous leprosy were selected for the study. The average age of the patients was 79.5 years old, with a range of 55 to 98 years. As a control group, 15 autopsy cases of non-leprosy patients were retrieved from the Department of Human Pathology, Kagoshima University (n = 13) and from the Department of Pathology, Imakiire General Hospital (n = 2). The average age of the control patients was 74.5 years old, with a range of 60 to 84 years old. For the neurologic complications and association of tuberculosis, we reviewed the autopsy records and searched the clinical information. In doubtful cases we carefully checked the patients' clinical charts from the hospital records.

All hematoxylin and eosin-stained sections were reviewed. For cases with obvious morphologic changes (vacuolar changes of neurons) in both the medulla oblongata (MO) and spinal cord (SC) (n = 19), cases without any morphologic changes (n = 8) and control cases (n = 10 for MO and SC, and n = 5 for SC and dorsal root ganglia) (Table 1), the following experiments were performed. Sections of the MO and SC were cut into slides of 4-μm thickness for hematoxylin and eosin staining, Fite-Faraco acid-fast staining, immunohistochemistry, and a terminal deoxynucleotidyl transferase dUTP nick-end labeling assay, and serial sections of 10-μm thickness were mounted on membranes for laser-captured microdissection (Molecular Machines and Industries, Glattbrugg, Switzerland). Only specimens from 10 control cases were available for terminal deoxynucleotidyl transferase dUTP nick-end labeling staining. Additionally, specimens from dorsal root ganglia taken from lepromatous leprosy cases (n = 27 of 67, 7 from the study group listed in Table 1 and 20 from other cases) and those from control cases (n = 5) were examined for similar study.

Immunohistochemistry

Immunohistochemistry using the avidin-biotinylated enzyme complex (ABC) method was performed on the 4-μm sections. Mouse monoclonal antibody specific for PGL-I (clone DZ 2C11, dilution 1:1000; personally provided by Fujirebio Inc., Tokyo, Japan [14]) and anti-bacillus-Calmette-Guérin (anti-BCG) polyclonal antibody (rabbit anti-*Mycobacterium bovis*; DakoCytomation, Glostrup, Denmark, dilution 1:2000) were used as primary antibodies. Biotinylated horse anti-mouse IgG, biotinylated anti-rabbit IgG and avidin-biotinylated alkaline phosphatase (ABC-AP and Elite ABC-AP) were purchased from Vector Laboratories (Burlingame, CA) as the Vectastain ABC Kit (AK-5001) or the Vectastain Elite ABC Kit (AK-5002).

Staining Procedure

Immunohistochemical staining was performed using the ABC method, as described previously (15). Briefly, each section was deparaffinized, endogenous peroxidase was blocked by treatment with 0.3% hydrogen peroxide in methanol for 30 minutes, and then the section was re-hydrated. After washing with phosphate-buffered saline (PBS), sections were incubated with normal serum at room temperature for 30 minutes; normal horse serum in PBS and normal goat serum were used for PGL-I and BCG, respectively. This was followed by incubation with primary antibodies at room temperature for 1 hour for BCG and at 4°C for 16 hours for PGL-I antigen. After washing with PBS, the sections were incubated with the biotinylated secondary antibody (goat anti-rabbit IgG for BCG and horse anti-mouse IgG for PGL-I antigen) and then washed with Tris-buffered saline. Sections were then treated with ABC-AP reagent (BCG) or Elite ABC-AP reagent (PGL-I) for 30 minutes. After washing, samples were visualized using fuchsin as a substrate and counterstained with hematoxylin. Specimens of *Mycobacterium tuberculosis* (from five human lung tissues of tuberculosis) and five different strains of *Mycobacterium ulcerans* (from mouse foot pad) were used as controls to test the specificity of the PGL-I staining.

Laser-Captured Microdissection

Membrane-mounted 10-μm sections were stained with hematoxylin and dried in an incubator to ensure thorough drying. The regions in the serial sections corresponding to the area where immunohistochemistry was performed (nucleus ambiguus and spinal anterior horn cells) were selected with UV laser-captured microdissection using a Nikon AU2000 (Nikon, Tokyo, Japan).

DNA Extraction

DNA extraction was performed using a DNeasy Tissue Kit (QIAGEN, Inc., Valencia, CA) according to the manufacturer's instruction. Briefly, the microdissected tissues were mixed with 180 μL of ATL buffer and 20 μL of Proteinase K, mixed thoroughly by vortexing, and incubated at 55°C overnight. AL buffer was added, and the mixture

was incubated at 70°C for 10 minutes to denature proteinase. The sample was then frozen at −20°C for 1 hour, thawed at room temperature, and then mixed with 200 μL of ethanol and centrifuged for 1 minute. The sample was washed with 500 μL of AW1 washing buffer and centrifuged for 1 minute, and then 500 μL of AW2 buffer was added and the sample was centrifuged for 3 minutes at 14,000 rpm. Finally, the sample was washed with AE buffer, and DNA was extracted. The preparation was stored at 4°C.

Polymerase Chain Reaction Amplification

Clean, protective clothing along with frequent glove changes and all other necessary precautions were taken to avoid cross-contamination of polymerase chain reaction (PCR) products. A nested PCR for *M. leprae* genomic DNA was performed by modification of the method of Donoghue et al (16). PCR was performed using a GeneAmp PCR System 2400 (PerkinElmer), with primers targeted to the *M. leprae* repetitive sequence RLEP yielding a 129-bp outer product and a 99-bp nested product.

Oligonucleotides Used as Polymerase Chain Reaction Primers

The following primers were used: LP-1, 5′-TGCAT GTCATGGCCTTGAGG-3′; LP-2, 5′-CACCGATAC CAGCGGCAGAA-3′;LP-3,5′-TGAGGTGTCGGCGTG GTC-3′; and LP-4,5′-CAGAAATGGTGCAAGGGA-3′ (16). The outer primers LP-1 and LP-2 and the inner primers LP-3 and LP-4 were bought from Sigma-Genosys (Ishikari, Japan). The PCR mixture was taken from a ExTaq HotStart kit (TaKaRa Bio Inc., Shiga, Japan): each PCR mixture contained 5 μL of genomic DNA, 1.25 units of TaKaRa ExTaq HS (TaKaRa), 10x ExTaq buffer, 2.5 mM dNTP mixture, and 50 pmol sense and antisense primers in a volume of 25μL. The PCR conditions were an initial cycle at 94°C for 4 minutes, followed by 30 cycles at 94°C for 40 seconds, 58°C for 1 minute, and 72°C for 30 seconds, with a final extension reaction at 72°C for 1 minute in the first PCR. The product of the first PCR (0.5 μL) was used as a template for a second PCR, in which 25 cycles of the same PCR conditions were used. The specificity of the PCR primers (LP1, LP2, LP3, and LP4) was tested with specimens of *M. tuberculosis* DNA (extracted from human lung tissue) and five different strains of *M. ulcerans* DNA (extracted from mouse foot pads) as controls.

Gel Electrophoresis

Gel electrophoresis was performed on a 1.5% agarose gel. The PCR product (10 μL) was added to 2 μL of loading buffer, and electrophoresis was performed in TBE buffer in two stages of 35 V for 5 minutes and 135 V for 18 minutes. Amplified DNA was visualized by ethidium bromide and UV light. A 50-bp ladder marker (Invitrogen) was used as a size marker.

Nucleotide Sequencing of Amplified DNA

The amplified DNA band was cut from the agarose gel under UV illumination and purified using a QIAquick PCR purification kit (QIAGEN) according to the manufacturer's instructions. Nucleotide sequencing was performed using an ABI Model 3700 (Version 3.7) automated sequencer (Applied Biosystems, Foster City, CA).

Terminal Deoxynucleotidyl Transferase Biotin-dUTP Nick-End Labeling Staining

A terminal deoxynucleotidyl transferase biotin-dUTP nick-end labeling (TUNEL) assay was performed using an Apoptag Kit (S7110, Intergen, Purchase, NY). Paraffin sections were deparaffinized, treated with 20 μg/mL Proteinase K, and then with 3% hydrogen peroxide in PBS to quench endogenous peroxide, before being washed two times with distilled water. Equilibration buffer was added, and the mixture was incubated with a working solution of terminal deoxynucleotidyl transferase for 1 hour at 37°C. Stop/wash buffer was then applied at room temperature for 10 minutes. The sections were washed three times in PBS, anti-digoxigenin conjugate was added, and the mixture was incubated at room temperature for 30 minutes in a humidified chamber. After washing four times with PBS and color development with a peroxidase substrate, the specimens were washed three times with distilled water and counterstained with methyl green.

Statistics

Statistical analysis was performed using a Mann-Whitney U test and χ^2 test to compare quantitative data populations with non-normal distributions or unequal variance. A value of $p < 0.05$ was considered to be statistically significant.

RESULTS

Clinical Findings

The majority of he patients showed evidence of neurologic complications such as bending of the fingers, shortening of the extremities, lagophthalmos, and/or blindness. These features were recorded according to World Health Organization (WHO) disability grading (17): 97% (65 of 67) had grade 2 disability, and 3% (2 of 67) were free from disability (grade 0). No clinical evidence of bulbar palsy was noted. Signs of motor neuron disease or cranial neuropathies were not recorded in the clinical records except for case 13, who showed marked muscular atrophy of the extremities resembling motor neuron disease, but this patient showed no respiratory muscle weakness.

Histologic Findings

Of the 67 leprosy cases, 44 (67%) were found to have vacuolar changes of motor neurons either in the MO (nucleus ambiguus or hypoglossal nucleus) (Fig. 1A, B) or SC (anterior horn neurons in the cervical, thoracic, and lumber cords), and 19 of 67 cases (28%) had positive vacuolar changes in both the MO and SC. The cervical (29%) and lumber (32%) cords showed more vacuolar changes than the thoracic cord (8%). The neurons were swollen and showed foamy changes; although the normal shape was preserved for some neurons, the whole cytoplasm of others had been replaced by tiny vacuoles (Fig. 1C). No

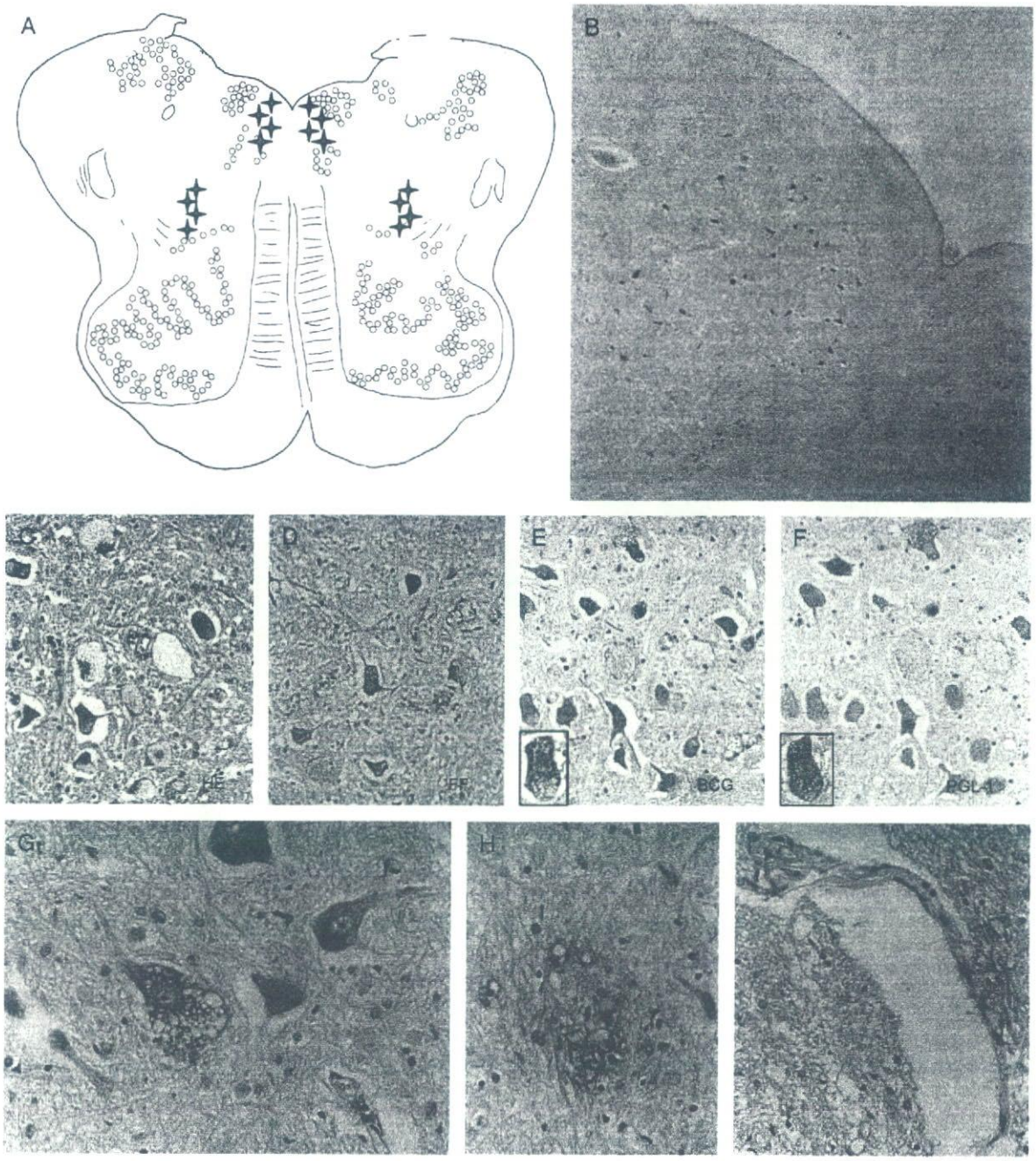

FIGURE 1. Histopathologic and immunohistochemical findings in the brainstem and spinal cord in lepromatous leprosy cases. **(A)** Distribution of phenolic glycolipid-I (PGL-I)-positive neurons in the medulla oblongata in lepromatous leprosy cases (red stars), indicating the nucleus ambiguous and hypoglossal nucleus. **(B)** PGL-I-positive neurons in the hypoglossal nucleus (original magnification: 50×). **(C–F)** Histopathologic changes in the nucleus ambiguous. **(C)** Swollen cells with vacuolated changes (hematoxylin and eosin; original magnification: 220×). **(D)** Negative results for acid-fast staining (Fite-Faraco; original magnification: 220×). **(E)** Positive results for anti-bacillus Calmette-Guérin (BCG) immunohistochemistry (BCG; original magnification: 220×); inset shows a BCG-positive neuron. **(F)** Positive results for leprosy-specific anti-PGL immunohistochemistry (PGL-I; original magnification: 220×); inset shows a PGL-I-positive neuron. **(G–I)** Histopathologic changes in the spinal cord. **(G)** Anterior horn motor neurons were swollen and showed foamy changes, although the normal shape of some neurons was preserved; the neurons were strongly positive for PGL-I (PGL-I; original magnification: 500x). **(H)** Vacuolated spaces in neuropils of the spinal cord (PGL-I; original magnification: 500×). **(I)** Vascular endothelial cells showing foamy changes and positive staining for PGL-I (original magnification: 500×).

TABLE 1. Summary of Histopathologic Findings and Polymerase Chain Reaction Results in Lepromatous Leprosy and Control Cases

			Medulla Oblongata					Spinal Cord					Dorsal Root Ganglion				
Case	Age (years)	Sex	HE	FF	PGL-I	BCG	DNA	HE	FF	PGL-I	BCG	DNA	HE	FF	PGL-I	BCG	DNA
1	63	M	VC+	−	+	+	+	VC+	−	+	−	+	[NA]				
2	78	F	VC+	−	+	+	+	VC+	−	+	+	+	[NA]				
3	79	M	VC+	−	+	+	+	VC+	−	+	+	+	[NA]				
4	81	M	VC+	−	+	+	+	VC+	−	+	+	+	[NA]				
5	81	M	VC+	−	+	+	+	VC+	−	+	+	+	[NA]				
6	82	M	VC+	−	+	+	+	VC+	−	+	+	+	[NA]				
7	86	M	VC+	−	+	+	+	VC+	−	+	+	+	[NA]				
8	75	M	VC+	−	+	+	+	VC+	−	+	+	−	[NA]				
9	82	M	VC+	−	+	+	+	VC+	−	+	+	−	[NA]				
10	98	F	VC+	−	+	+	+	VC+	−	+	+	−	[NA]				
11	55	M	VC+	−	+	+	−	VC+	−	+	+	+	[NA]				
12	71	F	VC+	−	+	+	−	VC+	−	+	+	+	[NA]				
13	74	M	VC+	−	+	+	−	VC+	−	+	+	+	VC+	−	+	+	+
14	79	M	VC+	−	+	+	−	VC+	−	+	+	+	[NA]				
15	80	M	VC+	−	+	+	−	VC+	−	+	+	+	VC+	−	+	+	+
16	81	M	VC+	−	+	+	−	VC+	−	+	+	+	[NA]				
17	82	M	VC+	−	+	−	−	VC+	−	+	+	+	[NA]				
18	90	M	VC+	−	+	+	−	VC+	−	+	+	+	VC+	−	+	+	−
19	92	M	VC+	−	+	+	−	VC+	−	+	+	−	[NA]				
20	82	F	VC−	−	−	+	+	VC−	−	+	−	+	[NA]				
21	67	F	VC−	−	−	−	−	VC−	−	+	+	+	VC+	−	+	+	−
22	73	M	VC−	−	+	−	−	VC−	−	+	+	+	VC+	−	+	+	−
23	79	F	VC−	−	−	−	−	VC−	−	+	+	+	VC−	−	−	−	−
24	81	F	VC−	−	−	+	−	VC−	−	+	+	+	[NA]				
25	63	M	VC−	−	+	−	−	VC−	−	+	+	−	[NA]				
26	84	M	VC−	−	−	−	−	VC−	−	+	+	−	VC+	−	+	−	−
27	84	M	VC−	−	−	+	−	VC−	−	−	−	−	[NA]				
C-1	72	F	VC−	−	−	−	−	VC−	−	−	−	−	[NA]				
C-2	73	M	VC−	−	−	−	−	VC−	−	−	−	−	[NA]				
C-3	73	M	VC−	−	−	−	−	VC−	−	−	−	−	[NA]				
C-4	74	F	VC−	−	−	−	−	VC−	−	−	−	−	[NA]				
C-5	74	M	VC−	−	−	−	−	VC−	−	−	−	−	[NA]				
C-6	74	F	VC−	−	−	−	−	VC−	−	−	−	−	[NA]				
C-7	75	M	VC−	−	−	−	−	VC−	−	−	−	−	[NA]				
C-8	78	M	VC−	−	−	−	−	VC−	−	−	−	−	[NA]				
C-9	79	F	VC−	−	−	−	−	VC−	−	−	−	−	[NA]				
C-10	84	M	VC−	−	−	−	−	VC−	−	−	−	−	[NA]				
C-11	66	M	[NA]					VC−	−	−	−	−	VC−	−	−	−	−
C-12	71	M	[NA]					VC−	−	−	−	−	VC−	−	−	−	−
C-13	60	F	[NA]					VC−	−	−	−	−	VC−	−	−	−	−
C-14	80	M	[NA]					VC−	−	−	−	−	VC−	−	−	−	−
C-15	84	F	[NA]					VC−	−	−	−	−	VC−	−	−	−	−

HE, hematoxylin and eosin; FF, Fite-Faraco acid-fast staining; PGL-I, phenolic glycolipid-I; BCG, bacillus-Calmette-Guérin; M, male; F, female; VC, vacuolar changes; [NA], not available; +, positive; −, negative; C-1–C-15, control cases.

acid-fast organisms were present based on the results of Fite staining (Fig. 1D). However, immunohistochemically the neurons were positive for BCG and *M. leprae*-specific PGL-I antigen (Fig. 1E, F). Most cases showed strong staining intensity, and almost all vacuolated neurons and spaces were PGL-I-positive; the staining showed an intracytoplasmic vacuolar and granular pattern. Many neurons also contained a large amount of lipofuscin pigments. Because alkaline phosphatase with fuchsin was used to visualize the samples, the neurons positive for *M. leprae* antigen stained red, whereas the neurons with lipofuscin pigment remained brown. Some neurons showed a mix of red and brown colors due to the presence of both mycobacterial materials and lipofuscin pigments (Fig. 1G). Small vacuolated changes

TABLE 2. Correlation of Hand and Foot Deformity and Vacuolar Changes in Spinal Anterior Neurons

	Gr0*	Gr2	Gr4
Vacuolar changes −	6	2	28
Vacuolar changes +	0	9	22

*, Modified World Health Organization (WHO) disability grading: Gr0, WHO grade 0, Gr2; WHO grade 2 in hands or feet; Gr4, WHO grade 2 in both hands and feet ($p = 0.04$).

were also detected in neutrophils (Fig. 1H), but macrophage granuloma formation was not observed and no hyperplasia or hypertrophy of capillary endothelial cells was found. In 2 cases, vacuolated changes were noted in vascular endothelial cells, and these cells were positive for PGL-I (Fig. 1I). In the dorsal root ganglia, 21 of 27 cases of leprosy showed vacuolated neurons and 22 of 27 were positive for PGL-I immunostaining. All the above findings were negative in the 15 control cases. Specimens of 5 lung tissues of tuberculosis

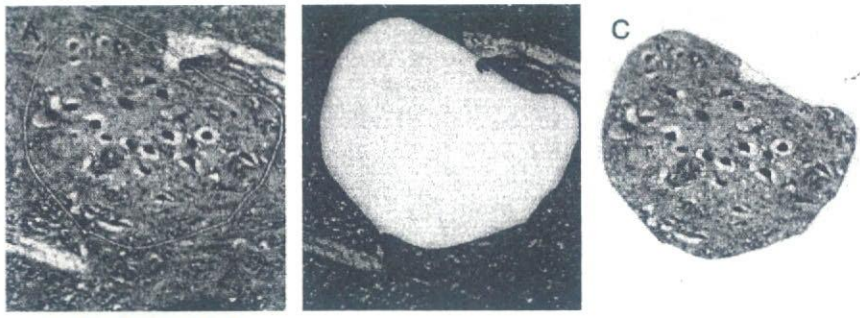

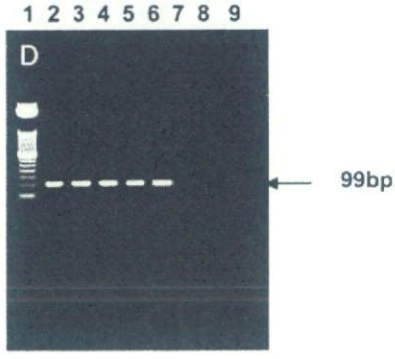

E

M. leprae RLEP	TGAGGTGTCGGCGTGGTCAATGTGGCCGCACCTGAACAGGCACGTCCCCGTGCACGG
Case 3 MO	TGAGGTGTCGGCGTGGT-CAATGTGGCCGCACCTGAACAGGCACGTCCCCGTGCACGG
Case 3 SC	TGAGGTGTCGGCGTGGT-CAATGTGGCCGCACCTGAACAGGCACGTCCCCGTGCACGG
Case 4 MO	TGAGGTGTCGGCGTGGTTCAATGTGGCCGCACCTGAACAGGCACGTCCCCGTGCACGG
Case 4 SC	TGAGGTGTCGGCGTGGT-CAATGTGGCCGCACCTGAACAGGCACGTCTCCGTGCACGG
Case 20 MO	TGAGGTGTCGGCGTGGT-CAATGTGGCCGCACCTGAACAGGCACGTCCCCGTGCACGG
Case 20 SC	TGAGGTGTCGGCGTGGT-CAATGTGGCCGCACCTGAACAGGCACGCCCCCGTGCACGG

M. leprae RLEP	TATAACTATTCGCACCTGATGTTATCCCTTGCACCATTTCTG
Case 3 MO	TATAACTATTCGCACCTGATGTTATCCCTTGCACCATTTCTG
Case 3 SC	TATAACTATTCGCACCTGATGTTATCCCTTGCACCATTTCTG
Case 4 MO	TATAACTATTCGCACCTGATGTTATCCCTTGCACCATTTCTG
Case 4 SC	TATAACTATTCGCACCTGATGTTATCCCTTGCACCATTTCTG
Case 20 MO	TATAACTATTCGCACCTGATGTTATCCCTTGCACCATTTCTG
Case 20 SC	TATAACTATTCGCACCTGATGTTATCCCTTGCACCATTTCTG

FIGURE 2. Molecular analysis of microdissected specimens. **(A–C)** Laser-capture microdissection of the nucleus ambiguus, showing an original section **(A)**, a dissected residual tissue **(B)**, and a tissue for DNA extraction **(C)**. **(D)** Detection of *M. leprae*-specific DNA in the human central nervous system by nested polymerase chain reaction (PCR). *M. leprae*-specific DNA was amplified from the medulla oblongata (MO) and spinal cord (SC) of lepromatous leprosy cases but not from control cases (lane 1, 50-bp marker; lane 2, positive control for *M. leprae* DNA; lane 3, MO from a case with vacuolated changes; lane 4, SC from a case with vacuolated changes; lane 5, MO from a case without vacuolated changes; lane 6, SC from a case without vacuolated changes; lane 7, MO from a control non-leprosy case; lane 8, SC from a control non-leprosy case; and lane 9, negative control). **(E)** DNA sequence homology of PCR products showing 99% to 100% sequence homology between the detected sequences. First line, *M. leprae* repetitive sequence RLEP3 from the National Center for Biotechnology Information database X17153; second to fifth lines, MO and SC from Case 3 and Case 4 (cases with vacuolated changes); sixth and seventh lines, MO and SC from Case 20 (case without vacuolated changes).

TABLE 3. TUNEL-Positive (Apoptotic) Neurons in the Nucleus Ambiguus and Spinal Cord in Disease and Control Cases

Cases	Age (years)	Gender	TUNEL-Positive/Total Identified Neurons, n (%)	
			Medulla Oblongata	Spinal Cord
1	63	M	0/15 (0)	NA
2	78	F	1/35 (2.86)	7/128 (5.47)
3	79	M	1/32 (3.13)	9/159 (5.66)
4	81	M	0/27 (0)	0/190 (0)
5	81	M	NA	2/183 (1.09)
6	82	M	0/18 (0)	3/89 (3.37)
7	86	M	0/23 (0)	NA
8	75	M	1/32 (3.13)	0/19 (0)
9	82	M	0/8 (0)	0/40 (0)
10	98	F	0/14 (0)	1/175 (0.57)
11	55	M	0/43 (0)	4/96 (4.17)
12	71	F	0/0 (0)*	0/182 (0)
13	74	M	0/45 (0)	3/155 (1.94)
14	79	M	0/40 (0)	1/133 (0.75)
15	80	M	0/29 (0)	2/113 (1.77)
16	81	M	0/4 (0)	3/121 (2.48)
17	82	M	2/15 (13.3)	16/106 (15.09)
18	90	M	NA	NA
19	92	M	0/24 (0)	1/73 (1.37)
20	82	F	0/5 (0)	1/30 (3.33)
21	67	F	2/16 (12.5)	11/52 (21.15)
22	73	M	1/31 (3.2)	6/254 (2.36)
23	79	F	0/47 (0)	2/191 (1.05)
24	81	F	0/16 (0)	3/62 (4.84)
25	63	M	0/0 (0)*	0/30 (0)
26	84	M	0/3 (0)	11/166 (6.63)
27	84	M	0/6 (0)	0/40 (0)
C-1	72	F	0/0 (0)*	0/95 (0)
C-2	73	M	0/20 (0)	1/141 (0.71)
C-3	73	M	0/3 (0)	9/163 (5.52)
C-4	74	F	1/20 (5)	3/107 (2.80)
C-5	74	M	0/22 (0)	9/96 (9.38)
C-6	74	F	0/33 (0)	8/104 (7.69)
C-7	75	M	0/21 (0)	0/61 (0)
C-8	78	M	0/10 (0)	0/116 (0)
C-9	79	F	0/18 (0)	0/95 (0)
C-10	84	M	0/24 (0)	0/58 (0)
C-11	66	M	NA	NA
C-12	71	M	NA	NA
C-13	60	F	NA	NA
C-14	80	M	NA	NA
C-15	84	F	NA	NA

*, No identified neurons in the nucleus ambiguus area in serial sections.
TUNEL, terminal deoxynucleotidyl transferase biotin-dUTP nick-end labeling; M, male; F, female; C1–C15, control cases, NA, not available.

and 5 strains of *M. ulcerans* from mouse were also negative for PGL-I staining.

As shown in Table 1, PGL-I immunostaining was positive in the MO and SC in all cases with vacuolated changes (19 of 19). In cases without obvious vacuolated changes, PGL-I was positive in the MO in 2 of 8 cases (25%, $p < 0.001$) and in the SC in 7 of 8 cases (88%, not significant). In total, *M. leprae*-specific PGL-I antibody was identified in the MO in 21 of 27 cases (78%), whereas the SC was positive for PGL-I in 26 of 27 of cases (96%).

Neuronal loss was evaluated by counting the number of spinal anterior horn neurons from leprosy cases and age-matched control cases. Cervical and lumbar cords were counted separately (cervical cord of leprosy [n = 22], 56.3 ± 30.8; cervical cord of control [n = 6], 48.0 ± 27.6; lumbar cord of leprosy [n = 22], 64.5 ± 28.9; lumbar cord of control

[n = 10], 71.1 ± 28.9). There was no statistically significant neuronal loss between leprosy and control cases by Mann-Whitney U test (cervical, p = 0.67; lumbar, p = 0.24).

Correlation Between Clinical Findings and Histologic Findings

As shown in Table 2, there was a statistically significant correlation between hand and foot deformity grading and the presence of vacuolar changes in spinal anterior horn neurons (p = 0.04).

Polymerase Chain Reaction Analysis

Representative data from microdissected specimens of the nucleus ambiguus in the MO are shown in Figure 2A–C. PCR analysis revealed positive amplification of *M. leprae*-specific genomic DNA in 18 of 19 cases (95%) with obvious histologic changes in both the MO and SC and in 5 of 8 cases (63%) without vacuolated changes (Table 1). *M. leprae* DNA was identified in the MO in 11 of 27 cases (41%) and in the SC in 20 of 27 cases (74%) (Fig. 2D). In the dorsal root ganglia, *M. leprae*-specific DNA was identified in 5 of 27 cases (18.5%) of leprosy. DNA sequencing results (Fig. 2E) demonstrated more than 99% homology with *M. leprae*-specific genomic sequences obtained from a BLAST search of the gene database of the National Center for Biotechnology Information. The control non-leprosy cases were negative in the PCR analysis. PCR of specimens of 5 lung tissues of tuberculosis and 5 strains of *M. ulcerans* from mouse was repeated 5 times. Among 5 tuberculosis specimens, 2 were completely negative (0/5), but 3 sometimes showed positive bands (2/5, 3/5, and 3/5). Also among 5 *M. ulcerans* specimens, one was completely negative (0/5), but 4 showed positive bands (2/5, 2/5, 2/5, and 3/5) (Supplementary Fig. 1).

Correlation Between Immunohistochemistry and Polymerase Chain Reaction

A statistical analysis was performed, including the 10 control cases, and the following results were obtained: in the MO, PGL+ and DNA+, n = 10; PGL− and DNA+, n = 1; PGL+ and DNA−, n = 11; PGL− and DNA−, n = 15 (χ^2 test, $p < 0.02$); and in the SC, PGL+ and DNA+, n = 20; PGL− and DNA+, n = 0; PGL+ and DNA−, n = 6; PGL− and DNA−, n = 11 (χ^2 test, $p < 0.001$).

Terminal Deoxynucleotidyl Transferase Biotin-dUTP Nick-End Labeling

A TUNEL assay was performed to determine whether damaged motor neurons in lepromatous leprosy cases were undergoing apoptosis (Table 3). More TUNEL-positive (apoptotic) cells (8 of 528 neurons, 1.5%) were found in the nucleus ambiguus of leprosy cases than in control non-leprosy cases (1 of 179 neurons, 0.6%), but these data did not show a statistically significant difference (χ^2 and Mann-Whitney U test). Except for one neuron (Fig. 3A), apoptosis was not observed in vacuolated neurons of the nucleus ambiguus. The TUNEL-positive cells were mostly atrophic, and some were filled with lipofuscin pigment. Similar findings were observed in spinal anterior horn motor neurons (Fig. 3B), and apoptosis was noticed mostly in the olive nucleus and the inferior vestibular nucleus (N VIII) (Fig. 3C). The TUNEL-positive neurons (Fig. 3A–C) had eccentrically located and pyknotic nuclei, but typical apoptotic bodies were not found. TUNEL-positive cells in non-leprosy cases showed a similar staining pattern. The anterior motor neurons of the spinal cord showed no significant difference in apoptosis between leprosy cases (75 of 2,732 neurons, 2.7%) and non-leprosy cases (30 of 1,036 neurons, 2.8%). However, in TUNEL-positive cases, the percentage of DNA fragmentation in lepromatous cases

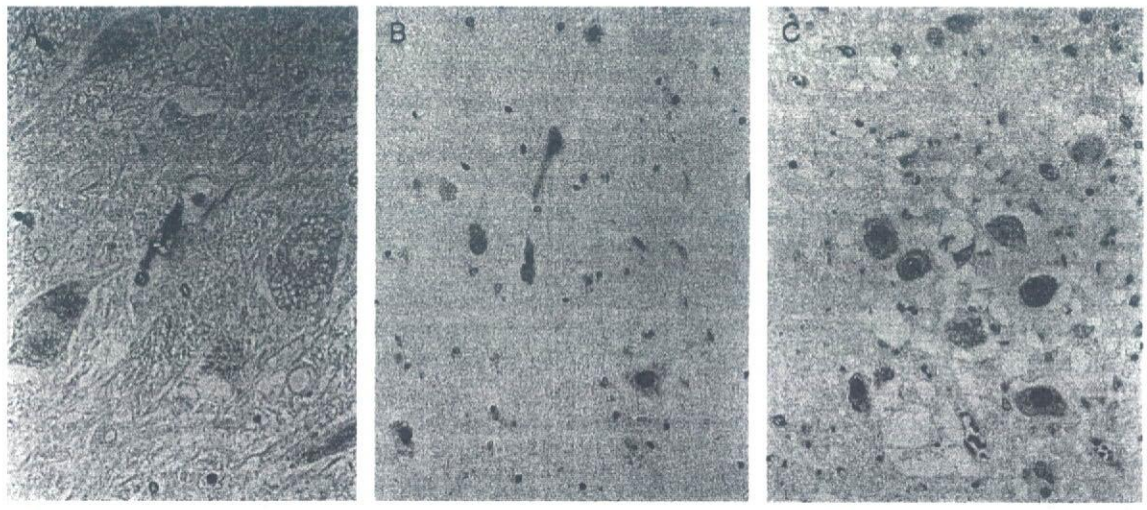

FIGURE 3. Representative images from terminal deoxynucleotidyl transferase biotin-dUTP nick-end labeling (TUNEL) staining of neuronal apoptosis in lepromatous leprosy cases, showing eccentrically placed and pyknotic nuclei. **(A)** TUNEL-positive neuron in the nucleus ambiguus with vacuolated changes (original magnification: 385×). **(B)** TUNEL-positive neurons in the spinal anterior horn (original magnification: 350×). **(C)** TUNEL-positive neurons in the inferior vestibular nucleus (original magnification: 385×).

(2.9%–13% in the MO and 0.6%–21% in the SC) was relatively high compared with DNA fragmentation in control cases (5% in the MO and 0.7%–9% in the SC). The autopsy records showed the median duration of formalin fixation for the specimens were 10 days for leprosy cases and 9.5 days for control cases. As internal controls, endothelial cells were positively stained in all cases. However, a negative association between the fixation period and TUNEL labeling results ($p < 0.001$) was observed.

DISCUSSION

Our immunohistochemical data show the presence of mycobacterial antigens in neurons of the CNS in cases of leprosy. Glycolipids from the cell wall of *M. leprae* are widely distributed in the tissue of patients with leprosy, and among these PGL-I is known to be specific to *M. leprae* and not found in other mycobacterial species (18). PGL-I is a phenolic-diacylphthiocerol trigycerides and forms a loose capsule around the bacillus (19). There are high levels of antibodies to PGL-I in sera of highly bacillated lepromatous leprosy patients compared with those in less bacillated tuberculoid leprosy patients and in healthy individuals. Lepromatous leprosy patients who become smear-negative after treatment show a decreased level of these antibodies (20). However, treated patients still frequently harbor a significant level of antibodies to PGL-I (21), and PGL-I is detectable by immunohistochemistry in tissue sections from leprosy specimens (22, 23). Antigens have been identified in intracytoplasmic bacillary staining with solitary, granular, and debris patterns and in soluble antigenic staining in a vacuolar or amorphous pattern (22). Positive PGL-I immunostaining in Buruli ulcer caused by *M. ulcerans*has also been reported (24), although we recently showed a PGL-I-negative result in mouse *M. ulcerans* lesions (15).

Katoch et al (25) have reviewed the evidence for clinical involvement of cranial nerves V, VII, and VIII in leprosy, and pointed out that the CNS may be involved in the disease. Dhar et al (26) reported multiple cranial neuropathies involving cranial nerves VII, IX, X, and XII in leprosy, and Gopinath et al (27) also discussed the involvement of cranial nerves VII, I, V, and VIII in a clinical study. However, involvement of the nuclei of these cranial nerves in leprosy has yet to be confirmed. Our results show that *M. leprae*-specific PGL-I antigen is expressed in motor neurons of the spinal cord at all levels (cervical, thoracic, and lumber) and in the nucleus ambiguus in the MO. Expression of PGL-I antigen in the hypoglossal nucleus, its fascicle, and the inferior and lateral vestibular nuclei was also observed in some cases, and immunoreactivity to PGL-I antigen was seen in cell bodies of the anterior horn motor neurons and in the neuropils. The vacuolar and intracytoplasmic granular staining patterns observed in the present study are also compatible with previous work (23). Patil et al (28) also reported on detection of *M. leprae*-specific PGL-I antibodies and protein components in the cerebrospinal fluid of 33 lepromatous leprosy patients. Eleven of their patients had clinical signs and symptoms of CNS involvement, which suggested an association between the presence of these antibodies and upper motor neuron signs.

All our cases were long-term cured leprosy cases (disease-free for more than 10 years and slit skin smear-negative), and therefore only dead organisms were thought to be present in the CNS. This may explain the lack of acid fastness, although conversion to the non-acid fast, cell wall-deficient dormant form found in *M. tuberculosis* may also have occurred (29), and the negative results in Fite staining support this theory. Highly sensitive methenamine silver stain for *M. leprae* was performed according to the modified Harada method (30). Control tuberculosis lung cases and lepromatous leprosy skin cases stained well and identified *M. tuberculosis* and *M. leprae* bacilli, respectively. However, in CNS specimens of lepromatous leprosy cases, motor neurons were not stained by this method, and only doubtful staining of fragmented bacilli was identified in endothelial cells, which were also positive for PGL-I (data not shown). Although evidence of morphologic changes due to *M. leprae* in motor neurons, endothelial cells, and neuropils was observed, there was no evidence for the macrophage granuloma formation seen in active infection induced by direct inoculation of bacilli into the brain in animal models in rat (31) and armadillo (32).

The presence of *M. leprae*-specific genomic DNA was further confirmed by nested PCR. In addition to the histopathologic and immunohistochemical findings, the DNA analysis confirms the persistence of *M. leprae* in the CNS even after long-term clinical cure; this is the first demonstration of this phenomenon. The *M. leprae* DNA in long-term treated cases is likely to be degraded or fragmented, and therefore the primers used in PCR were targeted to small-sized DNA fragments specific for the *M. leprae* RLEP sequence. This sequence is repeated 37 times in the *M. leprae* chromosome (33) and PCR using primers amplifying the RLEP repetitive sequence are 1,000-fold more sensitive than primers targeting the 36-kDa antigen (16); it has been shown that such primers can detect *M. leprae* DNA that is damaged or present at very low levels (34). The PCR products in this study were shown to be 99% to 100% homologous to the *M. leprae* RLEP3 sequence. A BLAST search of LP1, LP2, LP3, and LP4 showed no homology to other mycobacteria, and Kang et al (34) also confirmed the *M. leprae* specificity of LP1/LP2. *M. leprae* specificity of the PCR primers (LP1, LP2, LP3, and LP4) was further tested with specimens of *M. tuberculosis* DNA from human lung tissue and five different strains of *M. ulcerans* DNA from mouse footpads. They were mostly negative, but positive bands were sometimes obtained in repeated experiments. The possibility of the presence of sequences similar to our RLEP primers in *M. tuberculosis* and *M. ulcerans* genomes cannot be excluded, although such homology data were not obtained by a BLAST homology search.

The more frequent identification of *M. leprae* DNA in the SC (74%) than in the MO (41%) suggests that *M. leprae* reaches the CNS through upward invasion from the periphery to the central region through motor axons. The more common occurrence of vacuolated changes in anterior horn cells of the cervical and lumber cords than in the

thoracic cord also suggests that bacterial invasion may occur through the extremities rather than through the trunk of the patient. The presence of *M. leprae* antigen in vestibular nucleus XII may also account for the bulbar palsy that is sometimes seen in patients with lepromatous leprosy (4).

TUNEL staining identified DNA fragmentation in some neurons, but nuclear fragmentation with typical apoptotic bodies was not found. In addition, the pattern of distribution of DNA fragmentation in the brainstem and spinal cord was similar among long-term cured lepromatous leprosy patients and non-leprosy patients. Davison et al (35) pointed out that the duration of formalin fixation affects the detection of apoptosis in human brain specimens. We also examined the fixation period and found a negative correlation between the fixation period and TUNEL positivity, although endothelial cells were positively stained in all the cases, and the median fixation period was almost identical in both groups. We cannot conclude that vacuolar degeneration of motor neurons in the spinal cord and medulla oblongata was due to apoptosis by our present analyses.

M. leprae is thought to grow in low-temperature organs such as the skin, nasal cavity, testes, and anterior part of eye (36), and in animal models the growth is optimal between 27 and 30°C (37). Therefore, the CNS seems not to be the preferable site of growth. However, it is also known that in advanced cases *M. leprae* can grow in bone marrow (38), liver (39), and spleen (40), where body temperature is as high as that in the CNS.

The route of entry of *M. leprae* into motor neurons has not yet been proven. In viral infections, neural spread may occur as retrograde spread or anterograde spread (41). If we consider the retrograde spread pathway, *M. leprae*, which invaded into axons at the periphery of motor nerves (42–44), may move upward to the neuronal cell bodies. Instead, if anterograde spread exists, *M. leprae* invading sensory nerve axons may move to dorsal root of spinal cord, invade the dendrites of the motor neurons, and then finally reach the motor neuron cell bodies. We should also consider the possibility of hematogenous spread, as proposed by Scollard et al (45) for peripheral neuropathy. Positive PGL-I staining in the endothelium of the MO and SC in heavily infected cases may support this possibility. Further studies to identify the clues of *M. leprae* infections in various sites such as spinal roots and blood vessels are expected.

Recently, there has been growing interest in the role of autophagic stress in neuronal injury and degeneration. It is suggested that in the presence of impaired transport, fusion or degradative efficiency contributes to autophagic stress. In a mouse model of Alzheimer disease, an early axonopathy develops far in advance of other disease-related pathologic changes and implicates deficits in microtubule-dependent transport as a key pathogenic factor (46). Whether the vacuolated changes observed in motor neurons of lepromatous leprosy were due to similar mechanisms of axonopathy remains to be studied.

In conclusion, our results confirm that there is clear morphologic change in motor neurons of both the brainstem and anterior horn cells of the spinal cord in leprosy patients associated with the presence of PGL-I and mycobacterial DNA. Further investigation is required to correlate this finding to motor dysfunction and silent neuropathy in leprosy.

ACKNOWLEDGMENTS

The authors thank Dr. Y. Tashiro for provision of two autopsy samples for the control group. We are also grateful to Ms. T. Hatanaka, Mr. Y. Atsuji, Ms. Y. Arimura, and Ms. Y. Nishimura for their excellent technical assistance.

REFERENCES

1. *Global Leprosy Situation, 2005: Weekly Epidemiological Record 80.* Geneva, Switzerland: World Health Organization, 2005:289–95
2. *Leprosy Elimination Project, Status Report 2003.* Geneva, Switzerland: World Health Organization, 2004
3. Koya G, Arakawa I. Pathology of spinal cord in leprosy. Nippon Rai Gakkai Zasshi 1979;48:27–36
4. Hirai M, Sasaki N, Namba M. Leprous bulbar palsy (Seventh Joint Leprosy Research Conference) (Abstract). Int J Lepr Other Mycobact Dis 1972;40:461–62
5. Yamada N. Histopathological investigation of central nervous system in leprosy. I. Distribution of para-rosanilin-positive materials in leprosy with special relation to tissue injury. Nippon Rai Gakkai Zasshi 1984; 53:67–80
6. Harada K. A modified allochrome procedure for demonstrating mycobacteria in tissue sections. Int J Lepr Other Mycobact Dis 1977; 45:49–51
7. Mitsuda K. Atlas of leprosy. In: *Papers of Leprosy,* Vol VI. Kyoto, Japan: Nankodo, 1952
8. Goto M, Minauchi Y, Nobuhara Y, et al. Immunohistochemical demonstration of *Mycobacterium leprae* in the nervous system of long-term cured leprosy patients using a *M leprae* specific anti-PGL antibody. Jap J Trop Med Hyg 1993;21:117–21
9. Bryceson A, Pfaltzgraff RE. Complications due to nerve damage. In: *Leprosy.* Edinburgh, UK: Churchill Livingstone, 1979:77–88
10. Srinivasan H, Gupte MD. Experiences from studies on quiet nerve paralysis in leprosy patients. In: Antia NH, Shetty VP, eds. *The Peripheral Nerve in Leprosy and Other Neuropathies.* Delhi, India: Oxford University Press, 1997:30–35
11. Kaur G, Girdhar BK, Girdhar A, et al. A clinical, immunological, and histological study of neuritic leprosy. Int J Lepr Other Mycobact Dis 1991;59:385–91
12. Duncan ME, Pearson JM. Neuritis in pregnancy and lactation. Int J Lepr Other Mycobact Dis 1982;50:31–38
13. van Brakel WH, Khawas IB. Silent neuropathy in leprosy: An epidemiological description. Lepr Rev 1994;65:350–60
14. Fujiwara T, Minagawa F, Sakamoto Y, et al. Epitope mapping of twelve monoclonal antibodies against the phenolic glycolipid-1 of *M leprae.* Int J Lepr Other Mycobact Dis 1997;65:477–86
15. Goto M, Nakanaga K, Aung T, et al. Nerve damage in *Mycobacterium ulcerans*-infected mice: Probable cause of painlessness in Buruli ulcer. Am J Pathol 2006;168:805–11
16. Donoghue HD, Holton J, Spigelman M. PCR primers that can detect low levels of *Mycobacterium leprae* DNA. J Med Microbiol 2001;50: 177–82
17. WHO Expert Committee on Leprosy. *Sixth Report, 768. WHO Technical Report Series.* Geneva, Switzerland: World Health Organization, 1988
18. Brennan PJ, Barrow WW. Evidence for species-specific lipid antigens in *Mycobacterium leprae.* Int J Lepr Other Mycobact Dis 1980;48: 382–87
19. Koticha KK. *Leprosy: A Concise Text.* Bombay, India: Darshan K Koticha, 1990
20. Brett SJ, Draper P, Payne SN, et al. Serological activity of a characteristic phenolic glycolipid from *M leprae* in sera from patients with leprosy and tuberculosis. Clin Exp Immunol 1983;52:271–79
21. Gelber RH, Li F, Cho SN, et al. Serum antibodies to defined carbohydrate antigens during the course of treated leprosy. Int J Lepr Other Mycobact Dis 1989;57:744–51

22. Goto M, Izumi S. Light and electron microscopic immunohistochemistry using anti PGL-I antibody specific for *Mycobacterium leprae* (Abstract). Int J Lepr Other Mycobact Dis 1991;59:195
23. Wang T, Izumi S, Butt KI, et al. Demonstration of PGL-I and LAM-B antigens in paraffin sections of leprosy skin lesions. Nippon Rai Gakkai Zasshi 1992;61:165–74
24. Mwanatambwe M, Yajima M, Etuaful S, et al. Phenolic glycolipid-I (PGL-I) in Buruli ulcer lesions: First demonstration by immunohistochemistry. Int J Lepr Other Mycobact Dis 2002;70:201–5
25. Katoch K, Ramu G, Sengupta U, et al. Central nervous system involvement in leprosy. Indian J Lepr 1984;56:813–18
26. Dhar S, Sharma VK, Kaur S. Facial, glossopharyngeal, vagus and hypoglossal nerve palsy in a case of lepromatous leprosy. Indian J Lepr 1993;65:333–36
27. Gopinath DV, Thappa DM, Jaishankar TJ. A clinical study of the involvement of cranial nerves in leprosy. Indian J Lepr 2004;76:1–9
28. Patil SA, Katoch K, Ramu G, et al. Detection of antibodies against phenolic glycolipid-1 (PGL-1), 35-kDa and 30-40 kDa components of *Mycobacterium leprae* in the cerebrospinal fluid of leprosy patients. J Med Microbiol 1995;43:115–19
29. Chandrasekhar S, Ratnam S. Studies on cell-wall deficient non-acid fast variants of *Mycobacterium tuberculosis*. Tuber Lung Dis 1992;73: 273–79
30. Kawatsu K, Izumi S, Yumi M, et al. Modification of Harada's method for rapid staining of mycobacteria. Nippon Rai Gakkai Zasshi 1991;61: 175–81
31. Alamdarov IN. Cerebral changes in experimental rat leprosy (Abstract). Int J Lepr 1965;33:259
32. Job CK, Sanchez RM, Hastings RC. Lepromatous meningoencephalitis in the nine-banded armadillo (*Daspus novemcinctus*). Int J Lepr Other Mycobact Dis 1988;56:291–95
33. Cole ST, Supply P, Honoré N. Repetitive sequences in *Mycobacterium leprae* and their impact on genome plasticity. Lepr Rev 2001;72: 449–61
34. Kang TJ, Kim SK, Lee SB, et al. Comparison of two different PCR amplification products (the 18 kDa protein gene vs. RLEP repetitive sequence) in the diagnosis of *Mycobacterium leprae*. Clin Exp Dermatol 2003;28:420–24
35. Davison FD, Groves M, Scaravilli F. The effects of formalin fixation on the detection of apoptosis in human brain by in situ end-labelling of DNA. Histochem J 1995;27:983–88
36. Desikan KV, Job CK. A review of post-mortem findings in 37 cases of leprosy. Int J Lepr Other Mycobact Dis 1968;36:22–44
37. Shepard CC. Temperature optimum of *Mycobacterium leprae* in mice. J Bacteriol 1965;90:1271–75
38. Suster S, Cabello-Inchausti B, Robinson MJ. Non-granulomatous involvement of the bone marrow in lepromatous leprosy. Am J Clin Pathol 1989;92:797–801
39. Chen TSN, Drutz DJ, Whelan GE. Hepatic granulomas in leprosy. Arch Pathol Lab Med 1976;100:182–85
40. Benard JC, Vozquez CAJ. Visceral lesions in lepromatous leprosy: A study of 60 necropsies. Int J Lepr Other Mycobact Dis 1973;41:94–101
41. Flint SJ, Enquist LW, Krug RM, et al. Viral pathogenesis. In: Flint SJ, et al., eds. *Principles of Virology: Molecular Biology, Pathogenesis, and Control.* Washington, DC: ASM Press, 2000:595–628
42. Job CK, Verghese R. Electron microscopic demonstration of Myco leprae in axons. Lepr Rev 1974;45:235–39
43. Yoshizumi MO, Asbury AK. Intra-axonal bacilli in lepromatous leprosy: a light and electron-microscopic study. Acta Neuropathol (Berl) 1974;26:257–70
44. Chun LT, Zong-Min J, Skinsnes OK. Light and electron-microscopic study of *M leprae* infected armadillo nerves. Int J Lepr Other Mycobact Dis 1989;57:65–72
45. Scollard DM, McCormick G, Allen J. Localization of *Mycobacterium leprae* to endothelial cells of epineural and perineural blood vessels and lymphatics. Am J Pathol 1999;154:1611–20
46. Chu CT. Autophagic stress in neuronal injury and disease. J Neuropathol Exp Neurol 2006;65:423–32

JOURNAL OF CLINICAL MICROBIOLOGY, Nov. 2007, p. 3840–3843 Vol. 45, No. 11
0095-1137/07/$08.00+0 doi:10.1128/JCM.01041-07

"*Mycobacterium ulcerans* subsp. *shinshuense*" Isolated from a Skin Ulcer Lesion: Identification Based on 16S rRNA Gene Sequencing▽

Kazue Nakanaga,[1]* Norihisa Ishii,[1] Koichi Suzuki,[1] Kazunari Tanigawa,[1] Masamichi Goto,[2] Tsutomu Okabe,[3] Hideaki Imada,[4] Akemi Kodama,[5] Tomotada Iwamoto,[6] Hiroshi Takahashi,[7] and Hajime Saito[8]

Leprosy Research Center, National Institute of Infectious Diseases, Higashimurayama-shi, Tokyo, Japan[1]; Department of Human Pathology, Kagoshima University Graduate School of Medical and Dental Sciences, Sakuragaoka, Kagoshima, Japan[2]; Department of Dermatology, National Hospital Organization, Higashi-Hiroshima Medical Center, Higashi-Hiroshima, Japan[3]; Department of Orthopedic Surgery, National Hospital Organization, Higashi-Hiroshima Medical Center, Higashi-Hiroshima, Japan[4]; Department of Laboratory Medicine, National Hospital Organization, Higashi-Hiroshima Medical Center, Higashi-Hiroshima, Japan[5]; Department of Microbiology, Kobe Institute of Health, Kobe, Japan[6]; Stanford University Medical Center, Clinical Laboratories, Palo Alto, California[7]; and Hiroshima Environment and Health Association, Hiroshima, Japan[8]

Received 22 May 2007/Returned for modification 12 July 2007/Accepted 11 September 2007

We describe the fourth reported case involving "*Mycobacterium ulcerans* subsp. *shinshuense*." Compared to previous cases, the infection was more invasive with extensive ulceration from the elbow to the forearm. Definitive identification involved IS*2404* detection, 16S rRNA gene sequencing, and analysis of the 16S rRNA gene 3′-terminal region and the virulence plasmid pMUM001.

CASE REPORT

On 28 December 2005, a 20-year-old Japanese woman experienced painful swelling, marked by redness, extending from the right elbow to the forearm. As the condition persisted, the patient was seen on 6 January 2006 at the Department of Dermatology, National Hospital Organization, Higashi-Hiroshima Medical Center. On the first examination, marked swelling from the right elbow to the forearm and crusted ulceration, 1 cm in diameter, surrounded by redness and swelling of the right elbow, were observed. On 8 January, the patient was admitted and placed on a parenteral course of ampicillin-sulbactam and clindamycin. The treatment was changed to minocycline on 15 January as a result of increased severity of symptoms. As the magnetic resonance image was suggestive of a potential intramuscle abscess, the patient was transferred to orthopedic surgery where, on 23 January, a 15-cm incision was made and the affected area was cleansed with irrigation. No muscle involvement was evident at the time of the incision. While the patient's condition initially improved, an exacerbation occurred in early February. On 10 February, Ziehl-Neelsen staining of material from the ulcerated area revealed the presence of acid-fast bacilli (AFB) in clumps as well as dispersed. Purulent exudate taken from the ulcer was inoculated into a BBL MGIT (Becton Dickinson, Franklin Lakes, NJ) tube and on two 2% Ogawa egg medium slants for incubation at 27 and 35°C. On the basis of the acid-fast stain result, the patient was placed on isoniazid, rifampin, and ethambutol therapy. The patient's condition continued to worsen with the ulceration growing to the size of the palm with undermined edges and a yellowish-white necrotic base. On 28 March, PCR testing of a biopsy sample targeting a *Mycobacterium leprae*-specific sequence was negative, while the sample was positive for insertion sequence IS*2404*, which raised the possibility of *Mycobacterium ulcerans* or "*Mycobacterium ulcerans* subsp. *shinshuense*" as the causative organism.

On 4 April, the ulcer as well as surrounding skin tissue extending 15 cm proximal and distal from the elbow was excised. Following extensive surgical removal of the epidermal, dermal, and subcutaneous skin layers, artificial dermis was placed as a template for dermal regeneration. With the generation of healthy granulation tissue, the freshly formed dermis was covered with ×1.5-meshed thin split-thickness autograft. The patient steadily improved and was discharged on 12 June.

PCR targeting IS*2404* specific for *M. ulcerans* (7) was first performed on a thin section of formalin-fixed paraffin-embedded skin sample taken on 23 January. Briefly, PCR using forward primer PU4F (5′-GCGCAGATCAACTTCGCGGT-3′) and reverse primer PU7R (5′-GCCCGATTGGTGCTCG GT CA-3′) (gene positions 548 to 567 and 702 to 683, respectively) was followed by electrophoresis on a 2% agarose gel and staining with ethidium bromide. A 154-bp PCR product matching *M. ulcerans* 97-107 (African strain), 5143 (Mexican strain), and 1615 (Malaysian strain) was detected (Fig. 1a). PCR testing of DNA extracted from a fresh skin biopsy specimen taken on 28 March confirmed the presence of IS*2404* (Fig. 1b, lane 9). Because of the typical irregular distribution of clumps of AFB in Buruli ulcer, the excised skin specimen taken on 4 April was serially sectioned into eight sections. Each section was screened for IS*2404* as well as stained with hematoxylin-eosin and the Fite stain using standard methods. The biopsy section

* Corresponding author. Mailing address: Leprosy Research Center, National Institute of Infectious Diseases, 4-2-1 Aoba-cho, Higashimurayama-shi, Tokyo 189-0002, Japan. Phone: 81-42-391-8211. Fax: 81-42-394-9092. E-mail: nakanaga@nih.go.jp.

▽ Published ahead of print on 19 September 2007.

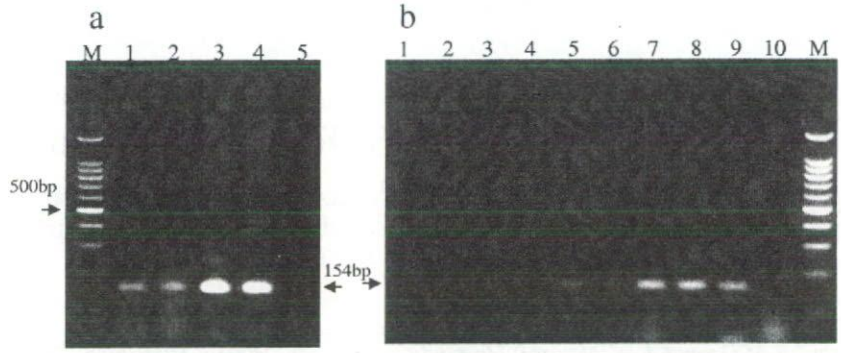

FIG. 1. PCR targeting IS*2404* specific for *M. ulcerans*. (a) Lane M, 100-bp ladder marker; lane 1, DNA sample extracted from paraffin-embedded skin (patient); lane 2, *M. ulcerans* 97-107 (African strain); lane 3, *M. ulcerans* 5143 (Mexican strain), lane 4; *M. ulcerans* 1615 (Malaysian strain); lane 5, negative control. (b) Lanes 1 to 8, DNA samples extracted from each of eight serially sectioned skin specimens taken on 4 April; lane 9, DNA sample extracted from a fresh skin biopsy specimen taken on 28 March; lane 10, negative control; lane M, 100-bp ladder marker.

strongly positive for the 154-bp product (Fig. 1b, lanes 7 and 8) corresponded with the presence of AFB on microscopy; however, weakly positive (lanes 5 and 6) and negative (lanes 1 to 4) sections were negative for AFB on microscopy. It is noteworthy that AFB was found within the deeper layers of the dermal tissue despite the normal appearance of the epidermis. AFB from the dermal and subcutaneous layer was purified and extracted. Two strains of "*M. ulcerans* subsp. *shinshuense*" and five strains of *M. ulcerans* (Table 1) were used as controls. Using previously described consensus primers, sequencing of almost the full length of the 16S rRNA gene was performed by direct sequencing of the PCR product with the ABI Prism 310 Genetic Analyzer (Applied Biosystems, Foster City, CA) (10). PCR primer pairs used were 5′-AGAGTTTGATCCTGGCT CAG-3′ (positions 8 to 27) and 5′-TGCACACAGGCCACA AGGGA-3′ (positions 1047 to 1028) in combination with 5′-GTGTGGGTTTCCTTCCTTGG-3′ (positions 830 to 849) and 5′-AAGGAGGTGATCCAGCCGCA-3′ (positions 1542 to 1523). Nucleotide numbering was based on *Escherichia coli* 16S rRNA gene sequence as reference. Sequence analysis was performed using DNASIS version 2.1 (Hitachi Software Engineering, Tokyo, Japan). The sequence of the 1,480-bp 16S rRNA gene obtained from the isolate in the present case was completely identical to "*M. ulcerans* subsp. *shinshuense*" strain 753 and "*M. ulcerans* subsp. *shinshuense*" ATCC 33728. At positions 54 to 510, the sequence of "*M. ulcerans* subsp. *shinshuense*" ATCC 33728 in the RIDOM database (15) was identical to that of our isolate and differed from *M. ulcerans* ATCC 19423 (type strain) and *Mycobacterium marinum* DSM44344 (type strain) by one base at position 492. As shown in Table 1, our isolate matched perfectly with the 16S rRNA gene 3′-end regions of "*M. ulcerans* subsp. *shinshuense*" reported by Portaels et al. (8) to be useful in discriminating "*M. ulcerans* subsp. *shinshuense*," three types of *M. ulcerans*, and *M. marinum*.

Finally, using primers for eight pMUM001 sequences coding for lipid toxin mycolactone-producing enzymes described by Stinear et al. (12), PCR products for our isolate, *M. ulcerans* 97-107 (African strain), and "*M. ulcerans* subsp. *shinshuense*" 753 were compared. As shown in Fig. 2, all eight bands were detected from the African strain, whereas "*M. ulcerans* subsp. *shinshuense*" 753 as well as our isolate lacked the band representing the serine/threonine protein kinase gene MUP011.

Of the specimens cultured for mycobacteria, our isolate was recovered from only the specimen taken on 10 February after 11 weeks of incubation at 27°C on a 2% Ogawa egg slant. All characteristics of our isolate with respect to IS*2404*, 16S rRNA genes, and pMUM001 were identical to data obtained from affected tissue samples that failed to yield mycobacteria on

TABLE 1. 16S rRNA gene sequences differentiating *M. ulcerans* and related species

Organism (origin)	Differing residue(s) (underlined) at position(s)[a]:			
	492	1247	1288	1449–1451
Mycobacterium sp. (patient)	TGGGGAA	GGTGCAA	TAAGGCC	ACCC---TTTG
"*M. ulcerans* subsp. *shinshuense*" 753 (Japan)	TGGGGAA	GGTGCAA	TAAGGCC	ACCC---TTTG
"*M. ulcerans* subsp. *shinshuense*" ATCC 33728	TGGGGAA	GGTGCAA	TAAGGCC	ACCC---TTTG
M. ulcerans Agy99 (Africa)	TGGAGAA	GGTGCAA	TAACGCC	ACCCTTTTTTG
M. ulcerans 1615 (Malaysia)	TGGAGAA	GGTGCAA	TAACGCC	ACCC---TTTG
M. ulcerans ATCC 19423[Tb]	TGGAGAA	GGTGCAA	TAACGCC	ACCC---TTTG
M. ulcerans 97-107 (Africa)	TGGAGAA	GGTGCAA	TAACGCC	ACCCTTTTTTG
M. ulcerans 5143 (Mexico)	TGGAGAA	GGTGCAA	TAAAGCC	ACCC---TTTG
M. marinum ATCC 927[Tc]	TGGAGAA	GGTACAA	TAAAGCC	ACC----TTTG

[a] Positions are based on *E. coli* 16S rRNA genes as the reference.
[b] Type strain of the species.
[c] Sequences are from database accession no. AF456240.

FIG. 2. PCR for the presence of the genes on pMUM001. DNA samples were extracted from *M. ulcerans* 97-107 (African strain) (a), "*M. ulcerans* subsp. *shinshuense*" 753 (b), and purified AFB from a skin specimen taken on 4 April (c). Lanes M, 100-bp ladder markers; lanes 1, *repA* (413 bp); lanes 2, *parA* (501 bp); lanes 3, serine/threonine protein kinase gene MUP011 (479 bp); lanes 4, loading domain of *mls* (560 bp); lanes 5, acyltransferase domain of *mls* (504 bp); lanes 6, *rep* type II thioesterase gene (500 bp); lanes 7, *rep* type III ketosynthase gene (496 bp);lanes 8, *rep* P450 hydroxylase gene (500 bp).

culture. Determination of cultural characteristics as well as identification procedures was performed as previously described (1). The isolate exhibited yellow, rough colonies with pigmentation when grown in the dark. The slowly growing mycobacterium formed visible colonies at 25 and 32°C on a 2% Ogawa egg slant but not at 37 and 42°C. No growth was seen on medium supplemented with 500 μg/ml *p*-nitrobenzonic acid or 5% NaCl. The isolate was negative for niacin, nitrate reduction, arylsulfatase (3 days), Tween 80 hydrolysis, pyrazinamidase, and iron uptake, while it was positive for catalase and 68°C catalase as well as urease. The in vitro antibiotic susceptibility of this isolate was determined by the microdilution method (16) using the BrothMIC NTM kit (Kyokuto Pharmaceutical Industrial Co. Ltd., Tokyo, Japan), with modification of the incubation temperature to 32°C. MIC testing was performed in triplicate on different days with two of three matching MICs used as the criteria for MIC determination. The MICs of the drugs tested were as follows: streptomycin, 0.25 μg/ml; ethambutol, 1 μg/ml; kanamycin, 0.25 μg/ml; isoniazid, 8 μg/ml; rifampin, ≤0.03 μg/ml; levofloxacin, 0.5 μg/ml; clarithromycin, 0.06 μg/ml; ethionamide, 8 μg/ml; amikacin, ≤0.5 μg/ml.

The taxonomic studies of Tsukamura and Mikoshiba on a mycobacterial strain isolated from the skin lesion of a 19-year-old Japanese woman established the existence of a mycobacterium resembling *M. ulcerans* which has been subsequently classified as "*M. ulcerans* subsp. *shinshuense*" (6, 13, 14). Since the initial report, a case involving this organism from China and another case from Japan have been reported (2, 5).

In the present case, the finding of AFB in the skin lesion raised the suspicion of *M. marinum*, *Mycobacterium haemophilum*, *M. ulcerans*, "*M. ulcerans* subsp. *shinshuense*," and *Mycobacterium leprae* as etiologic agents. Detection of IS*2404* from biopsy specimens taken at different times narrowed the etiology to *M. ulcerans* and "*M. ulcerans* subsp. *shinshuense*." The detection of IS*2404*, sequencing of 16S rRNA genes, the presence of genes on pMUM001, and the absence of the serine/threonine protein kinase gene MUP011 identified the organism as "*M. ulcerans* subsp. *shinshuense*." In the case of slow-growing, hard-to-isolate mycobacteria, biopsy followed by molecular diagnostics is the most timely and sensitive diagnostic approach for patient management decisions. As shown in this case report, culturing is not always reliable for some slow-growing mycobacteria and growth may take as long as 11 weeks.

This represents the fourth case of infection involving "*M. ulcerans* subsp. *shinshuense*," including the previous two cases in Japan. Compared to previous reports, this clinical case was more invasive as well as difficult to manage. The severity of the ulcerative lesion resembled Buruli ulcer, a recent *M. ulcerans* infection case report from Africa (9); however, based on 16S rRNA gene sequencing, our isolate was identical to "*M. ulcerans* subsp. *shinshuense*" ATCC 33728 and "*M. ulcerans* subsp. *shinshuense*" 753. Furthermore, of the eight pMUM001 gene sequences present in the plasmid responsible for the synthesis of mycolactone in *M. ulcerans* (11), the organism in this case report exhibited the same seven pMUM001 gene sequences found in the prototype "*M. ulcerans* subsp. *shinshuense*" strain (12). Moreover, phenotypic characteristics and in vitro drug susceptibilities were also consistent with those of the other three "*M. ulcerans* subsp. *shinshuense*" strains, including the isolate originated from China (2) (data not shown).

Because there were no apparent bacteriological differences to explain the virulence of the present isolate compared to the three other previously reported "*M. ulcerans* subsp. *shinshuense*" strains, we cannot explain why the isolate in this case was more invasive than those in previous cases. It is possible that the late administration of an effective drug(s) such as rifampin (MIC, ≤0.03 μg/ml), clarithromycin (MIC, 0.06 μg/ml), and/or amikacin (MIC, ≤0.5 μg/ml) resulted in a bacteriological cure but that the accumulation of the toxic lipid mycolactone led to the worsening of the lesion (3).

While "*M. ulcerans* subsp. *shinshuense*" has been rarely reported, there are several phenotypical and molecular differences between "*M. ulcerans* subsp. *shinshuense*" and *M. ulcerans* that should be noted (8, 12, 14). Of particular interest is the novel mycolactone produced by "*M. ulcerans* subsp. *shinshuense*" which resembles mycolactone A/B produced by *M. ulcerans* with only the side chain being structurally different as a result of changes in the coding region for biosynthesis of the side chain (4). Whereas these findings are not conclusive, they lead us to consider whether "*M. ulcerans* subsp. *shinshuense*" should be considered a "subspecies" of *M. ulcerans*. Additional studies may contribute to a better understanding of the evolutionary position as well as the geographical distribution of this organism.

REFERENCES

1. **Della-Latta, P., and I. Weitzman.** 1998. Mycobacteriology, p. 169–203. *In* H. D. Isenberg (ed.), Essential procedures for clinical microbiology, 1st ed. ASM Press, Washington, DC.
2. **Faber, W. R., L. M. Arias-Bouda, J. E. Zeegelaar, A. H. Kolk, P. A. Fonteyne, J. Toonstra, and F. Portaels.** 2000. First reported case of *Mycobacterium ulcerans* infection in a patient from China. Trans. R. Soc. Trop. Med. Hyg. **94:**277–279.
3. **George, K. M., D. Chatterjee, G. Gunawardana, D. Welty, J. Hayman, R. Lee, and P. L. Small.** 1999. Mycolactone: a polyketide toxin from *Mycobacterium ulcerans* required for virulence. Science **283:**854–857.
4. **Hong, H., J. B. Spencer, J. L. Porter, P. F. Leadlay, and T. Stinear.** 2005. A novel mycolactone from a clinical isolate of *Mycobacterium ulcerans* provides evidence for additional toxin heterogeneity as a result of specific changes in the modular polyketide synthase. Chem. Biol. Chem. **6:**643–648.
5. **Kazumi, Y., K. Ohtomo, M. Takahashi, S. Mitarai, I. Sugawara, J. Izumi, A. Andoh, and H. Hasegawa.** 2004. *Mycobacterium shinshuense* isolated from cutaneous ulcer lesion of right lower extremity in a 37-year-old woman. Kekkaku **79:**437–441.
6. **Mikoshiba, H., Y. Shindo, H. Matsumoto, M. Mochizuki, and M. Tsukamura.** 1982. A case of typical mycobacteriosis due to *Mycobacterium ulcerans*-like organism. Nippon Hifuka Gakkai Zasshi **92:**557–565.
7. **Phillips, R., C. Horsfield, S. Kuijper, A. Lartey, I. Tetteh, S. Etuaful, B. Nyamekye, P. Awuah, K. M. Nyarko, F. Osei-Sarpong, S. Lucas, A. H. Kolk, and M. Wansbrough-Jones.** 2005. Sensitivity of PCR targeting the IS*2404* insertion sequence of *Mycobacterium ulcerans* in an assay using punch biopsy specimens for diagnosis of Buruli ulcer. J. Clin. Microbiol. **43:**3650–3656.
8. **Portaels, F., P. A. Fonteyene, H. de Beenhouwer, P. de Rijk, A. Guedenon, J. Hayman, and M. W. Meyers.** 1996. Variability in 3′ end of 16S rRNA sequence of *Mycobacterium ulcerans* is related to geographic origin of isolates. J. Clin. Microbiol. **34:**962–965.
9. **Sizaire, V., F. Nackers, E. Comte, and F. Portaels.** 2006. *Mycobacterium ulcerans* infection: control, diagnosis, and treatment. Lancet Infect. Dis. **6:**288–296.
10. **Springer, B., W.-K. Wu, T. Bodmer, G. Haase, G. E. Pfyffer, R. M. Kroppenstedt, K.-H. Schröder, S. Emler, J. O. Kilburn, P. Kirschner, A. Telenti, M. B. Coyle, and E. C. Böttger.** 1996. Isolation and characterization of a unique group of slowly growing mycobacteria: description of *Mycobacterium lentiflavum* sp. nov. J. Clin. Microbiol. **34:**1100–1107.
11. **Stinear, T. P., A. Mve-Obiang, P. L. Small, W. Frigui, M. J. Pryor, R. Brosch, G. A. Jenkin, P. D. Johnson, J. K. Davies, R. E. Lee, S. Adusumilli, T. Garnier, S. F. Haydock, P. F. Leadlay, and S. T. Cole.** 2004. Giant plasmid-encoded polyketide synthases produce the macrolide toxin of *Mycobacterium ulcerans*. Proc. Natl. Acad. Sci. USA **101:**1345–1349.
12. **Stinear, T. P., H. Hong, W. Frigui, M. J. Pryor, R. Brosch, T. Garnier, P. F. Leadlay, and S. T. Cole.** 2005. Common evolutionary origin for the unstable virulence plasmid pMUM found in geographically diverse strains of *Mycobacterium ulcerans*. J. Bacteriol. **187:**1668–1676.
13. **Tsukamura, M., and H. Mikoshiba.** 1982. A new mycobacterium which caused skin infection. Microbiol. Immunol. **26:**951–955.
14. **Tsukamura, M., K. Kaneda, T. Imaeda, and H. Mikoshiba.** 1989. A taxonomic study on a mycobacterium which caused a skin ulcer in a Japanese girl and resembled *Mycobacterium ulcerans*. Kekkaku **64:**691–697.
15. **Turenne, C. Y., L. Tschetter, J. Wolfe, and A. Kabani.** 2001. Necessity of quality-controlled 16S rRNA gene sequence databases: identifying nontuberculous *Mycobacterium* species. J. Clin. Microbiol. **39:**3637–3648.
16. **Wallace, R. J., Jr., D. R. Nash, L. C. Steele, and V. Steingrube.** 1986. Susceptibility testing of slowly growing mycobacteria by a microdilution MIC method with 7H9 broth. J. Clin. Microbiol. **24:**976–981.

Title:

Efficacy of Recombinant BCG Vaccine Secreting IL-15/Ag85B fusion protein on Protection against *Mycobacterium tuberculosis*

Authors:

Ce Tang[1], Hisakata Yamada[1], Kensuke Shibata[1], Naoyoshi Maeda[2], Shinichi Yoshida[3], Worawidh Wajjwalku[4], Naoya Ohara[5], Atsushi Yamada[5], Taroh Kinoshita[6] and Yasunobu Yoshikai[1]

Affiliation:

[1]Division of Host Defense, Medical Institute of Bioregulation, Kyushu University, Fukuoka, Japan, [2]Digital Medicine Initiative, Kyushu University, [3]Department of Bacteriology, Kyushu University, [4]Department of Pathology, Faculty of Veterinary Medicine, Kasetsart University, Nakhonpathom, Thailand, [5]Division of Microbiology and Oral Infection, Department of Developmental and Reconstructive Medicine, Nagasaki University Graduate School of Biomedical Sciences, Nagasaki, Japan, [6]Department of Immunoregulation, Research Institute for Microbial Diseases, Osaka University, Osaka

Running title:

Efficacy of rBCG-IL15 against *M. tuberculosis*

Word count of the Abstract: 143 words

Word count of the Text: 3273 words

Footnotes:

[1]All the authors do not have a commercial or other association that might pose a conflict of interest.

[2]This work was supported by the Program of Founding Research Centers for Emerging and Reemerging Infectious Diseases and was launched as a project commissioned by the Ministry of Education, Culture, Sports, Science and Technology (MEXT), Japan by Grant-in-Aid for Japan Society for Promotion of Science, and grants from the Japanese Ministry of Education, Science and Culture (Y.Y.). [3]Information of this study has not been presented in any meeting.

[4]Correspondence and reprint requests to Dr. Yasunobu Yoshikai M.D. Ph.D., Division of Host Defence, Medical Institute of Bioregulation, Kyushu University, Fukuoka 812-8582, Japan Tel: +81-92-642-6972, Fax: +81-92-642-6973, E-mail: yoshikai@bioreg.kyushu-u.ac.jp

Abbreviations used in this paper: BCG, *Mycobacterium bovis* bacillus Calmette-Guérin; *M. tb*, *Mycobacterium tuberculosis*; TB, Tuberculosis; rBCG-Ag85B-IL15, recombinant BCG secreting antigen85B fused murine IL-15; Ab, antibody; i.p., intraperitoneally; i.t., intratracheally; PPD, purified protein derivative; Tc1, T cytotoxic 1; MNC, mononuclear cell; PEC, peritoneal exudates cells; CD62L, CD62 ligand; BMDC, bone marrow derived dendritic cell; LCMV, lymphocytic choriomeningitis virus.

Abstract

Protection against *Mycobacterium tuberculosis* depends on not only $CD4^+$ Th1 cells but also $CD8^+$ T cells. IL-15 has an important function in maintenance of memory $CD8^+$ T cells. In the present study, we examined the efficacy of recombinant *Mycobacterium bovis* Bacillus Calmette-Guérin (BCG) secreting fusion protein Ag85B/IL-15 (rBCG-Ag85B-IL15) in protection against *M. tuberculosis* infection. The levels of MHC class Ib (H2-M3)-binding TB-2- or MHC class Ia ($H\text{-}2D^b$)-binding MPT-64-specific $CD8^+$ T cells producing IFN-γ were significantly higher after immunization with rBCG-Ag85B-IL15 compared with rBCG-Ag85B. The levels of PPD- or Ag85B-specific $CD4^+$ T cells producing IFN-γ were also higher in rBCG-Ag85B-IL15-immunized mice than rBCG-Ag85B-immunized mice. The rBCG-Ag85B-IL15-immunized mice exhibited stronger $CD8^+$ and $CD4^+$ T cells responses and robust protection in lung against intratracheal challenge of *M. tuberculosis*. Thus, rBCG-Ag85B-IL15 vaccination capable of inducing efficient cell-mediated immunity might be used as an effective vaccine for tuberculosis.

Keywords:

T cells; Cytotoxic; Th1; Bacterial; Lung; Memory